Climate Dynamics (2004) 23: 63–78
DOI 10.1007/s00382-004-0422-0

E. Xoplaki · J. F. González-Rouco · J. Luterbacher
H. Wanner

Wet season Mediterranean precipitation variability: influence of large-scale dynamics and trends

Received: 15 September 2003 / Accepted: 26 February 2004 / Published online: 22 June 2004

Abstract The influence of the large-scale atmospheric circulation at several tropospheric levels on wet season precipitation over 292 sites across the Mediterranean area is assessed. A statistical downscaling model is designed with an objective methodology based on empirical orthogonal functions and canonical correlation analysis (CCA) and tested by means of cross-validation. In all 30% of the total Mediterranean October to March precipitation variability can be accounted for by the combination of four large-scale geopotential height fields and sea level pressure. The Mediterranean sea surface temperatures seem to be less relevant to explain precipitation variability at inter-annual time scale. It is shown that interdecadal changes in the first CCA mode are related to variations in the North Atlantic Oscillation index and responsible for comparable time scale variations of the Mediterranean precipitation throughout the twentieth century. The analysis reveals that since the mid-nineteenth century precipitation steadily increased with a maximum in the 1960s and decreased since then. The second half of the twentieth century shows a general downward trend of 2.2 mm·month^{-1}·decade^{-1}.

1 Introduction

The understanding and quantification of climatic changes at the continental and regional scale is an important and uncertain issue within the global change debate. A step towards a better understanding of impacts and regional climatic changes is the assessment of the characteristics of natural climate variability (e.g. Giorgi 2002a, b). Recent studies have revealed that the twentieth century was characterised by significant precipitation trends that can be observed at the global and the hemispheric scale with considerable variability on different time scales (e.g. Nicholls et al. 1996; Easterling et al. 2000; Folland et al. 2001; New et al. 2001).

The Mediterranean is one of the regions where the impacts of human-induced climate change are estimated to be high (Hulme et al. 1999). In the Mediterranean basin, future climate change is likely to aggravate significantly the existing problem of desertification and critically undermine the effectiveness of efforts to combat it.

Jacobeit (2000) and Giorgi (2002a) analysed the seasonal precipitation variability and trends over the Mediterranean land area for the period 1901–1998 based on the gridded (0.5° × 0.5° latitude-longitude) dataset of New et al. (2000). They found negative precipitation trends for winter in agreement with the findings of the IPCC (Folland et al. 2001). Many regional station-based studies find a similar decrease in precipitation in the western, central and eastern Mediterranean (e.g. Esteban-Parra et al. 1998; Piervitali et al. 1998; Türkes 1998; Kadioğlu et al. 1999; Buffoni et al. 1999, 2000; Xoplaki et al. 2000; González-Rouco et al. 2000, 2001; Tomozeiu et al. 2002; Xoplaki 2002).

The topography of the Mediterranean basin is complex with thermal and orographic forcing influencing the observed structure of weather systems and regional circulation (Fernández et al. 2003). The Mediterranean is a small-scale coupled atmosphere-ocean system with a rather short response time, thus regional long-term changes may be the result of changes in the more slowly responding global system.

One of the most critical aspects of the Mediterranean region is the hydrologic cycle and its variability in

E. Xoplaki (✉) · J. Luterbacher · H. Wanner
Institute of Geography, University of Bern,
Hallerstrasse 12, 3012 Bern, Switzerland
E-mail: elena.xoplaki@giub.unibe.ch

J. F. González-Rouco
Departamento de Astrofísica y Ciencias de la Atmósfera,
Universidad Complutense de Madrid, Madrid, Spain

J. Luterbacher · H. Wanner
NCCR Climate, University of Bern, Bern, Switzerland

relation to global climate variations and climate change. The balance between precipitation and evaporation influences the circulation and the quality of the waters in the Mediterranean Sea (e.g. Mariotti and Struglia 2002). The variability of the Mediterranean wet season precipitation influences the hydrological budget of the area and has an essential role in the management of regional agriculture, water resources, ecosystems, environment, economics as well as social development and behaviour.

Xoplaki (2002) found the months from October to March with highest precipitation amounts and high variability to be clearly the Mediterranean wet season. This is in agreement with Mariotti and Struglia (2002). The same definition has also been used by Eshel and Farrell (2000); Eshel et al. (2000); Eshel (2002) and Dünkeloh and Jacobeit (2003). This definition is valid for the Mediterranean region as a whole, however it is a compromise as smaller regional areas display different seasonality (Xoplaki 2002).

Despite the large spatio-temporal variability of precipitation, a significant fraction of its variation can be explained by large-scale circulation changes at different heights. Advective processes, especially during wintertime are an important factor controlling the regional changes of precipitation. Precipitation trends can further be associated with shifts in general atmospheric circulation features such as jet streams, storm tracks and monsoon circulations or with changes in the thermodynamic structure of the atmosphere (e.g. Eshel and Farrell 2000; Jacobeit 2000; Giorgi 2002a).

The tremendous importance of water availability in both ecosystems and societies underscores the necessity of understanding how a change in large-scale climate could affect rainfall variability as well as regional water supplies (e.g. Xu 1993; Rodrigo 2002; Knippertz et al. 2002). Thus, it is crucial to understand the relevant processes and physical mechanisms on different time scales as well as their link to the large-scale climate, which is responsible for the Mediterranean wet season precipitation variability and trend.

Many studies have related changes in Mediterranean precipitation regimes to the large-scale atmospheric circulation (e.g. Xoplaki 2002; Dünkeloh and Jacobeit 2003 and references therein). Several studies investigated the combined patterns of selected large-scale atmospheric fields and precipitation variability and aimed at explaining these connections in a physical sense (Zorita et al. 1992; Corte-Real et al. 1995; Reddaway and Bigg 1996; Eshel and Farrell 2000; Eshel et al. 2000; Quadrelli et al. 2001; Eshel 2002; Dünkeloh and Jacobeit 2003). As shown by Xoplaki et al. (2003a, b) and Matulla et al. (2003) the combination of various large-scale climate fields can account for a higher amount of explained variance of the local or regional climate fields than a single circulation parameter alone. Determination of the causes of the observed changes in Mediterranean precipitation over the last decades calls for improved understanding of the related changes which have taken place in atmospheric circulation.

This work attempts to further understanding of interannual to interdecadal Mediterranean precipitation variability and trend patterns during the wet season for the period 1950 to 1999 from the perspective of the changes in the large-scale dynamics. Implications for trends since the late nineteenth century are derived from this analysis as well as the performance of the NCEP reanalysis (Kalnay et al. 1996; Kistler et al. 2001) precipitation in reproducing some aspects of the variability found in the instrumental precipitation records analysed. Sea level pressure (SLP), sea surface temperature (SST) and geopotential height fields at several heights have been studied to assess their simultaneous relationship with Mediterranean recording station precipitation by means of an objective methodology. The large-scale predictors have been selected on the basis of previous studies (e.g. Zorita et al. 1992; Corte-Real et al. 1995; González-Rouco et al. 2000; Eshel et al. 2000; Rimbu et al. 2001) and because these variables are well simulated by atmosphere ocean global circulation models (AOGCMs; von Storch et al. 1993; Busuioc et al. 1999; González-Rouco et al. 2000). This enables future comparison work with downscaling experiments for scenario simulations (e.g. Cubasch et al. 2001; Gibelin and Déqué 2003). Moreover, this work could be of relevance for model validation exercises since reliability of model simulations at the regional scale is highly dependant on the correct characterisation of the large-scale patterns and their relation to the regional scale climate (e.g. González-Rouco et al. 2000).

Sections 2 and 3 briefly describe the datasets and the multivariate methods. Section 4 includes the results relating the combined information of large-scale anomaly fields of SLP and geopotential height to Mediterranean wet season precipitation using canonical correlation analysis in empirical orthogonal function space. The discussion and the conclusions are presented in Sect. 5 and 6, respectively.

2 Data

The following datasets have been used in this study: (1) monthly SLP as well as geopotential heights at different levels (850 hPa, 700 hPa, 500 hPa and 300 hPa) and precipitation were taken from the NCEP/NCAR reanalysis datasets (Kalnay et al. 1996; Kistler et al. 2001). SLP and geopotential heights have a resolution of 2.5°× 2.5° latitude-longitude, while precipitation is arranged in a T62 Gaussian grid (around 1.9° × 1.9° latitude-longitude). (2) monthly SST were taken from the Global Sea Ice Sea Surface Temperature, version 2.3b (GISST2; spatial resolution is 1° × 1° latitude-longitude) dataset (Rayner et al. 1996 updated). (3) monthly precipitation time series from 292 stations, distributed over the area 25°N–48°N and 10°W–45°E, including 30 countries along or close to the Mediterranean Sea, were collected (Fig. 1a). The same area was recently identified by Giorgi and Francisco (2000a, b) in their studies on evaluating uncertainties in the prediction of regional climate change. The data were

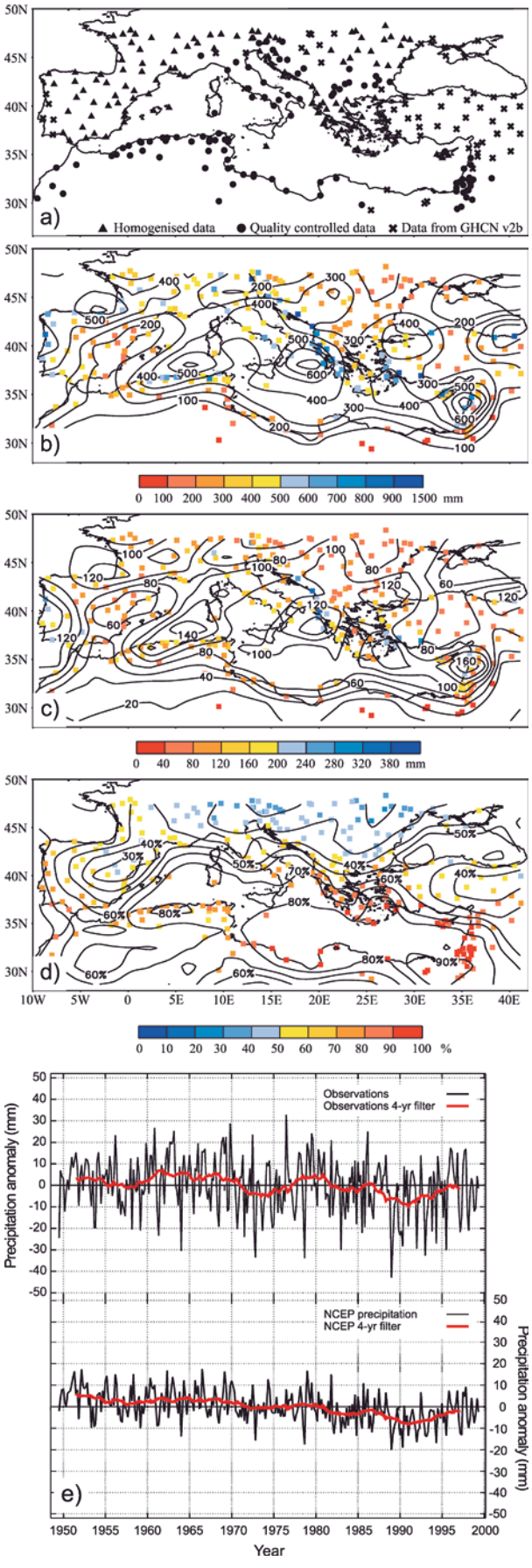

Fig. 1 Station precipitation time series and spatial and temporal characteristics of the Mediterranean wet season (ONDJFM) precipitation; 1950–1999. **a** Location of the 292 stations with continuous monthly time series of precipitation for the period October 1949 to March 1999. The stations are separated in to homogenised (*triangles*), quality controlled (*solid circles*) and GHCNv2b quality controlled (*crosses*) time series. **b** Wet season average precipitation amounts over the 292 Mediterranean sites (*coloured squares*) and the NCEP reanalysis gridded data (*contours*). **c** Wet season precipitation standard deviation based on the Mediterranean stations (*coloured squares*) and on the NCEP reanalysis data (*contours*). **d** Geographical distribution of the proportion (%) of wet season precipitation amounts to mean annual total over the larger Mediterranean area, 1950–1999 based on the Mediterranean stations (*coloured squares*) and on NCEP reanalysis data (*contours*). **e** *upper panel*: wet season precipitation anomalies averaged over the 292 sites (*black line*) and 4-year low pass filter (*red line*); *lower panel* wet season precipitation anomalies averaged over NCEP reanalysis data (*black line*) and 4-year low pass filter (*red line*)

obtained mainly from National Meteorological Services. The stations are separated by the level quality control applied to each series: Homogenised time series (by the National Meteorological Services; triangles), quality controlled (according to the guidelines of the WMO 1986; solid circles) and GHCN (Global Historical Climatology Network; Vose et al. 1992; Peterson et al. 1998; crosses) precipitation (version 2b) data. The latter provide detailed assessments of data quality, with rigorous quality control adjustments to decrease the effect of non-climatic factors on the time series.

Our analysis is restricted to the second half of the twentieth century (1950–1999) with good station coverage in the Mediterranean. Figure 1a presents the location of stations with continuous monthly records of precipitation for the period 1950–1999. The legend shows the type of pre-processing the data were subjected to by the source institutions (see Acknowledgements section).

In order to isolate the characteristics of the atmospheric variability concerning the larger Mediterranean area, a spatial window was defined, based on the highest correlation between the first principal component (PC1; 18.7% explained variance) of the wet season Mediterranean precipitation and the large-scale Northern Hemisphere geopotential height fields (Xoplaki et al. 2003a, b). It has been found that the geographical area spanning from 90°W to 90°E and 10°N to 80°N, including 2117 grid points, provides the most valuable atmospheric information connected to wet season precipitation over the larger Mediterranean area. To relate SST to the Mediterranean wet season precipitation, a spatial window with 1500 grid points covering the eastern North Atlantic, the Mediterranean and the Black Sea (29.5°W–44.5°E, 30.5°N–49.5°N) was used.

3 Methods

We follow the same approach as presented in Xoplaki et al. (2003a) assessing the connection between large-scale dynamics and Mediterranean surface air

temperature. Specifically, a downscaling model is calibrated using canonical correlation analysis (CCA) in the empirical orthogonal function (EOF) space and subsequently this model is validated by means of cross-validation. Only a short overview of the methods used are provided here, for a detailed description of the methodology the reader is referred to Xoplaki et al. (2003a, b); for an extended discussion about EOF, CCA and cross-validation see Barnett and Preisendorfer (1987), Michaelsen (1987), Wilks (1995) and von Storch and Zwiers (1999).

Before performing the CCA, the original data were projected onto their EOFs retaining only a limited number of them, accounting for most of the total variance in the datasets. As a preliminary step to the calculation of EOFs, the annual cycle was removed from all station and grid point time series by subtracting from each monthly value the respective month's 1950–1999 long-term mean. The gridded predictor data were then weighted by multiplying with the square root of the cosine of latitude to account for the latitudinal variation of the grid area (North et al. 1982; Livezey and Smith 1999).

A further step to ensure the stationarity of the variables needed for the calculation of EOFs and CCA was to detrend the time series. A standard linear least square fit method has been used as described e.g. by Edwards (1984). After the diagonalisation of the covariance and cross-correlation matrices during the EOF and CCA processes, the long-term trends were recovered by projecting (regressing) the original datasets onto their EOFs (canonical vectors) as in Busuioc and von Storch (1996), thus, providing estimations of the principal components and canonical series with long-term variability and trends.

In order to determine the most suitable number of EOFs to retain from each predictor field, two EOF analyses were applied. The first one selected as many components necessary to retain 90% of the variance of the original field. These merged principal components were used as input to a second EOF analysis in order to pick up the main modes of variation common to all predictor fields (Xoplaki et al. 2003a, b). A number of the resulting predictor principal components were selected to perform the CCA analysis in combination with the principal components of the predictand field.

In this work, we have taken the approach to retain the number of EOFs and canonical vectors, which leads to a better performance of the statistical models during cross-validation without over fitting the model. For the calculation of the EOF-CCA experiments, different numbers of EOFs have been considered, in both cases, for the predictor and predictand variables. The results of the selected single and multiple predictor models are presented in Table 1.

Two statistics were used in order to quantify and describe the skill of the canonical correlation model. These are the correlation skill score (ρ) and the Brier skill score (β) between the predictions (P) and the observations (O). The correlation provides a measure of concordance in the series and is given by: $\rho = Cov(P,O)/\sqrt{Var(P)\cdot Var(O)}$ as a function of the covariance (Cov) between predictions and observations and their respective variances (Var). The Brier score allows for a measure of explained variance, conventionally described as a relative probability score compared with the probability score of a reference forecast (see von Storch and Zwiers 1999 for a general definition and discussion). The reference forecast was based on climatology; β can then be defined as: $\beta = 1 - [Var(P-O)/Var(O)]$ where the last term indicates the ratio of the error variance relative to the variance of the observations. Thus, the Brier skill score with climatology as the reference is also the proportion of explained variance. For predictions with error variances in the order of the variance of the predictand, β will be close to zero or negative and for predictions with a relatively smaller amount of error, β tends to 1. Negative scores indicate that climatology is a better forecast than that suggested by the model.

4 Results

Figure 1b–e presents the wet season (ONDJFM) spatial and temporal distribution of precipitation over the larger Mediterranean area for 1950–1999. Precipitation statistics corresponding to the NCEP reanalysis (Kalnay et al. 1996; Kistler et al. 2001) are plotted along with station estimations for comparison reasons. The wet

Table 1 Summary of CCA results. Columns Predictor, X-EOFs and Y-EOFs: predictor variable(s), predictor(s) and predictand EOFs. X-Cum. Var. (%): percentage of accumulated predictor(s) EOFs variance. $CCAr_{1,2,3,4}$: canonical correlations for the first four modes. E.Var.1,2,3,4 (%): variance, each canonical mode accounts for, in the predictand. Tot.E.Var.1–4 (%): Total explained variance of the first four CCA pairs. ρ, β: correlations (ρ) and Brier score (β) from the cross-validation

Predictor	X-EOFs	Y-EOFs	X-Cum. Var. (%)	CCA r_1	CCA r_2	$CCAr_3$	$CCAr_4$	E.Var.1 (%)	E.Var.2 (%)	E.Var.3 (%)	E.Var.4 (%)	Tot. E. Var.1-4 (%)	ρ	β
300 hPa	12	12	88.3	0.90	0.87	0.81	0.67	16.2	9.9	5.6	5.6	26.9	0.43	0.21
500 hPa	12	12	89.9	0.90	0.88	0.79	0.69	16.3	9.7	5.4	6.3	27.1	0.43	0.20
700 hPa	12	12	91.6	0.91	0.87	0.77	0.73	16.2	9.8	5.4	6.1	27.3	0.42	0.20
850 hPa	12	12	92.5	0.91	0.86	0.79	0.72	16.2	9.5	5.5	5.9	27.1	0.42	0.20
SLP	12	12	91.3	0.92	0.81	0.82	0.71	16.1	8.4	6.8	5.6	26.5	0.42	0.20
SST	8	12	86.2	0.51	0.47	0.43	0.28	13.4	6.4	10.0	3.7	7.1	0.17	0.04
All fields	12	12	88.2	0.92	0.90	0.85	0.78	16.4	9.3	6.4	6.9	30.2	0.44	0.22

season precipitation map (Fig. 1b) shows a high spatial variability. Station ONDJFM averages show the lowest values in the desert areas of North Africa and the highest values in the eastern Adriatic coast over the Near East and along the western Iberian Peninsula.

Figure 1c shows the standard deviation pattern at the 292 sites (colour shading) and in the reanalysis data (contours). The spatial pattern of precipitation standard deviation shows a proportional relationship to the mean state: standard deviation values tend to be higher (lower) where the average values are also higher (lower). In general, there is good agreement between the large-scale structure of the spatial distribution shown in the observations and in the reanalysis data. The NCEP data captures the areas of maxima and minima of precipitation mean and variability, however it tends to underestimate local station precipitation values and their variability. The rainfall totals during the studied season (ONDJFM) constitute a very important proportion of the annual precipitation amounts in the area (Fig. 1d). The wet season amount varies between 30% (northwest Mediterranean area with continental climate) and 98% (eastern North Africa and Near East). The importance of the land-sea contrasts and orography is also highlighted by sharp gradients near the Mediterranean coast and larger features such as the Pyrenees area.

Figure 1d shows overall agreement between the instrumental observations and the reanalysis, both on the spatial distribution of the winter ratio of rainfall and in the amplitude. This plot suggests that even if the NCEP/NCAR reanalysis data underestimate the amplitude and variability of rainfall on the local scale, they tend to simulate in a realistic way the wet season proportion of rainfall.

Figure 1e shows the monthly time evolution of the spatially averaged precipitation anomalies both for the instrumental data (upper panel) and the reanalysis (lower panel); their 4-year moving average low pass filtered time series are also shown to aid comparison at longer time scales. There is good agreement between the NCEP and station data (correlation 0.78). The plot also highlights the underestimation of variability by the NCEP/NCAR reanalysis data: the ratio of variances observations versus NCEP is 3.11. Decadal changes show good agreement between both datasets in depicting relatively wet and dry periods (see filtered data): relative maxima take place in the early 1950s, 1960s, late 1970s to early 1980s and late 1990s while relative minima occur in the late 1950s, early 1970s and early 1990s. The decadal changes are superimposed upon a long term negative trend of 2.2 mm·month^{-1}·decade^{-1}(station data; 1.5 mm·month^{-1}·decade^{-1} for the reanalysis), significant at the 0.05 level.

4.1 CCA in EOF space

The different EOF-CCA-Cross-validation experiments are summarised in Table 1. In the columns titled Predictor, X-EOFs and Y-EOFS the different predictors as well as the number of predictor and predictand EOFs retained for each experiment, either unicomponent or multicomponent, are presented. The cumulative explained variance of the predictor field is given in the column X-Cum.Var. (%). The canonical correlations of the first four CCA pairs between the circulation and the wet season precipitation are contained in the columns CCA r_1, CCA r_2, CCA r_3 and CCA r_4, while the corresponding explained variance for the predictands is given in the columns E.Var.1, 2, 3, 4 (%). The column Tot. E.Var.1–4 (%) reveals the total explained variance, taking into consideration the first four canonical pairs. The last two columns present the performance of the models; in ρ, the correlation skill score and the Brier skill score β.

The connection between each single large-scale predictor field and the wet season precipitation are shown in the corresponding rows of Table 1 with the final row showing the combined influence of all five large-scale predictors.

4.2 Unicomponent EOF-CCA-cross-validation

The unicomponent EOF-CCA-cross-validation experiments with the wet season precipitation were performed retaining twelve EOFs for each of the single predictor fields (Table 1, X-EOFs). They account for between 88.3% (300 hPa) and 92.5% (850 hPa) of the total variance, whereas twelve EOFs of wet season precipitation account for 73.7%.

The single atmospheric predictors explain around 27% of total wet season precipitation variance each. A CCA model using only SST as predictor performs less well and accounts for only 7% of the total wet season Mediterranean precipitation variability. The models performance is presented in columns ρ and β with spatial averages of correlation and Brier skill scores obtained over all sites. The correlation between the cross-validated wet season precipitation totals and the raw data are significant at the 99% level ($n = 50 \times 6 = 300$ months, $r \geq 0.15$).

Cross-validation shows values of averaged spatial correlation and Brier score that go along with the amount of total explained variance by each large-scale field. The performance of SST is comparatively low (0.17 and 0.04 spatial correlation and Brier score, respectively). The relatively low values of ρ and β in Table 1, in comparison to Mediterranean summer temperature (Xoplaki et al. 2003a) suggest that precipitation shows less spatial averaged predictability. There are areas with good skill while in others the statistical model fails to reproduce the climate variability of precipitation.

4.3 Multicomponent CCA

CCA experiments with different numbers of X-EOFs, Y-EOFs and canonical pairs have been calculated and the performance of the models compared. Except for the

case of SST, results showed that the best performance of the models was achieved including more than 10 EOFs. Over this limit ρ and β tend to be stable with little variation that owing to minor changes in predictive skill in specific local regions. Heuristically we kept 12 X,Y-EOFs as a parsimonious reference model for each unicomponent case and for the multicomponent model for comparison reasons.

A clear gain in the total explained variance for the October-March precipitation is obtained from the multicomponent EOF-CCA (Tot. E.Var.1–4). Simultaneously, the model indicates a relatively better performance in cross-validation. More than 30% of the Mediterranean wet season precipitation can be explained by the combination of the five predictor fields. These results were not improved by including the Mediterranean SSTs as a sixth predictor.

Higher amounts of the wet season Mediterranean precipitation are explained by reducing the number of station time series of lower skill (not shown). When the southeastern most stations, where there is low model performance, are excluded, the averaged explained variance, skill and correlation are higher.

In general, the skill of the downscaling model depends on the chosen configuration in terms of the number of principal components and canonical modes selected (as well as other factors such as the spatial extension of the predictors) and on the potential predictability of local precipitation. The model presented herein shows improved skill when it is fitted using the sites that present higher predictability. Such models can be optimised for the regions where potential predictability is higher. Instead of showing the results of an approach that leads to optimal predictive power of the statistical model for certain Mediterranean areas, the discussion will be focused on the model which better fits the changes in precipitation in all stations throughout the period of study. The reason for this is to illustrate the spatial distribution of skill and clearly depict the areas where the statistical approach presented here gives less skilful results.

4.4 Maps of CCA results

The interannual covariability between the Mediterranean wet season precipitation and the combined large-scale circulation at different levels during the period 1950–1999 are presented here using the canonical patterns obtained in the multicomponent approach (All Fields Table 1).

The results will mainly focus on the first two CCA modes, since they capture most of the Mediterranean precipitation variability. Spatial patterns and expansion coefficients of these modes are presented in Figs. 2 and 4. The first CCA pair (Fig. 2) accounts for around 12% to 16% of the total wet season mean variance of each large-scale predictor and for 16.4% of the wet season precipitation variability, respectively. This pair exhibits a canonical correlation between the precipitation and the multicomponent field coefficient time series of 0.92. The canonical patterns of the geopotential height fields (Fig. 2a–e) present an equivalent barotropic structure throughout the entire troposphere with strong negative (positive) anomalies centred over northwestern Europe. The central and western Mediterranean lie at the southern margin of this anomaly pattern. A positive (negative) height anomaly centred north of the Caspian Sea covers the Eastern Mediterranean. The corresponding wet season precipitation anomaly pattern (Fig. 2f) indicates above (below) normal values almost over the entire basin, except for the southeastern Mediterranean.

The last graph in Fig. 2 presents the variations of the normalised monthly time components of the first CCA pair. The correlation between the precipitation canonical series and the Mediterranean wet season precipitation (Fig. 1e) is 0.72 (significant at the 0.05 level). Thus, it seems that there is a relevant contribution from this canonical mode to the long-term trends in wet season Mediterranean precipitation. Wet and dry periods agree well with those in Fig. 1e: wet half year periods in the 1960s, the end of 1970s and single years at the 1980s and 1990s; dry seasons are found during the 1950s, the first part of the 1970s, the end of the 1980s and beginning of the 1990s. The end of the 1980s and early 1990s in particular are well known for general drought conditions over large parts of the Mediterranean (Kutiel et al. 1996a; Eshel and Farrell 2000; Maheras 2000).

Figure 3 shows the regression maps between the first canonical series of precipitation (Fig. 2g) and SST (GISST) and precipitation (NCEP) fields for the 1950 to 1999 period. The SST regression pattern (Fig. 3a) reveals a configuration of anomalies largely in agreement with the barotropic behaviour pointed out earlier: positive (negative) SST anomalies lie below positive (negative) geopotential height anomalies. The precipitation regression pattern illustrates an expanded version of Fig. 2f. In general, positive precipitation anomalies appear in combination with moist advection to the land; negative precipitation anomalies occur in combination with continental outflow.

The second pair of wet season CCA (Fig. 4) (0.90 canonical correlation) explains 6.5% (SLP) to 8.5% (500 hPa geopotential) of the predictor variance and 9.3% of the Mediterranean wet season precipitation variability. The relevant tripole pattern of the geopotential height fields reveals a barotropic structure with a strong positive (negative) anomaly over the North Atlantic stretching towards the western Mediterranean. A second negative (positive) anomaly extends from southeastern Greenland over Scandinavia and eastern Europe to the eastern Mediterranean and North Africa at the upper tropospheric fields. In the positive phase, this constellation leads to anomalous northerly flow over the Iberian Peninsula and western North Africa and northwesterly flow over the central basin.

Except for the Iberian Peninsula, the remaining parts are influenced by an anomalous low-pressure system, with above-normal precipitation. The second pair of canonical series (Fig. 4g) shows intense negative anom-

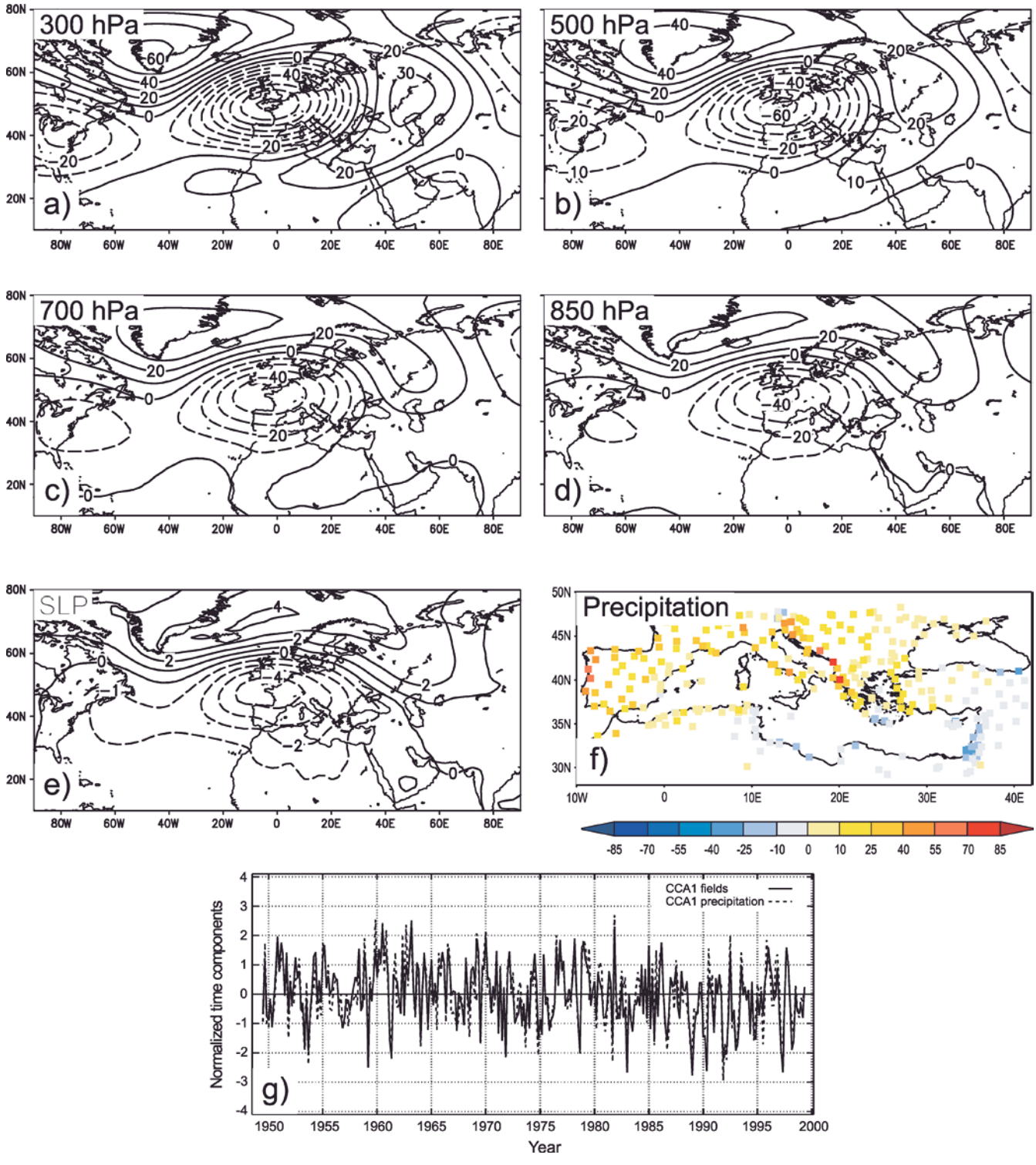

Fig. 2 Canonical spatial patterns of the first CCA. The canonical correlation patterns depict typical anomalies in the variables, with **a** 300 hPa; **b** 500 hPa; **c** 700 hPa; **d** 850 hPa; **e** SLP; **f** wet season precipitation anomalies in mm and **g** normalised time components of CCA1

alies in the wet seasons of 1964, 1972 and 1990, and positive in 1953, 1981 and 1999.

Figure 5 presents the regression patterns of SST and NCEP precipitation with the precipitation canonical series (Fig. 4g). The SST anomalies (Fig. 5a) underlie barotropically the geopotential anomalies. NCEP precipitation anomalies (Fig. 5b) agree on the large-scale with those of the station-derived pattern in Fig. 4f and are

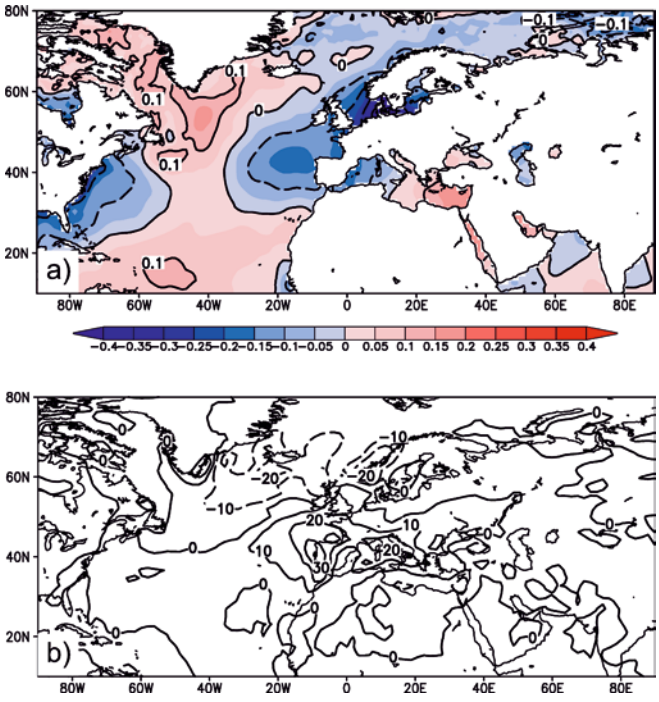

Fig. 3 Regression maps between the precipitation canonical series shown in Fig. 2g and **a** SST and **b** NCEP reanalysis precipitation for the same period

suggestive of advective processes: westerly and southwesterly winds from the Mediterranean sea induced by the low over Europe promote advection and orographic precipitation in the northeastern Mediterranean coasts.

Figure 6 shows the spatial distribution of skill in terms of ρ and β for the model based on five large-scale predictors. Both skill scores present a very similar spatial structure, with higher values in the western and northern Mediterranean where variances are higher (Fig. 1c).

5 Discussion

Regional or local climate is generally much more variable than climate on a hemispheric or global scale because variations in one region are compensated for by opposite variations elsewhere (e.g. Jones and Mann 2004). Indeed a closer inspection of the spatial structure of climate variability, in particular on seasonal and longer time scales, shows that it occurs predominantly in preferred large-scale and geographically anchored spatial patterns. Such patterns result from interactions between the atmospheric circulation and the land and ocean surfaces (IPCC 2001).

5.1 Mediterranean precipitation variability and the large-scale climate

The concurrent CCA relating the combination of five large-scale fields to October-March Mediterranean precipitation yielded physically meaningful pairs of patterns that accounted for 30% of overall precipitation variability. CCA1 in its positive phase is associated with positive rainfall anomalies over the western, central and northern Mediterranean area. Drier conditions prevail over the remaining region.

The highest precipitation anomalies in the CCA1 pattern are prevalent along the western side of the Dynarides and Pindos. Cyclones from the Gulf of Genoa steer southeastward through Italy, as for as to the Albanian and Greek coasts and then beyond to the southern coast of Turkey (Trigo et al. 1999; Karaca et al. 2000). They are reinforced as they move over the warmer Mediterranean and together with the orographical forcing cause high amounts of precipitation over these areas (e.g. Türkes 1998; Fotiadi et al. 1999; Kadioğlu 2000; Xoplaki et al. 2000). Our findings support the results of Zorita et al. (1992) who investigated the interaction between the winter atmospheric circulation, the SSTs in the North Atlantic area and the Iberian precipitation. In their first CCA between mean winter SLP and Iberian rainfall low SLP in the mid-Atlantic guides maritime air and precipitating weather systems into Iberia connected with decreasing anomalies towards the east.

These findings are also in agreement with the study of Corte-Real et al. (1995) on the linkages between the nonseasonal large-scale atmospheric circulation influence on precipitation over the Mediterranean area. A pattern similar to the first CCA 500 hPa anomaly field has been found by Quadrelli et al. (2001) for the period 1979–1995. They connect this pattern to the North Atlantic Oscillation (NAO; Hurrell 1995; Jones et al. 1997), the Arctic Oscillation (AO; Thompson and Wallace 1998) and the East Atlantic/Western Russia (EA/WRUS; EU2) pattern (Barnston and Livezey 1987).

The correlation between the coefficient time series of the first CCA of precipitation and the NAO (Jones et al. 1997) is –0.66, while with the AO and the EA/WRUS is –0.55 and –0.50, respectively.

Eshel and Farrell (2000) and Eshel et al. (2000) advanced a simple theory explaining winter (October-March) eastern Mediterranean rainfall variability in terms of subsidence anomalies associated with large-scale North Atlantic anomalies. Their concept of anomalous high pressure over Greenland/Iceland and an accompanied concurrent anomalous cyclone over the Mediterranean connected with anomalous warm southerlies, enhanced absent and higher precipitation amounts in the region is very similar to the structure of our first CCA of winter precipitation. Our 700 hPa to 300 hPa anomaly patterns indicate an increasing influence of a positive (negative) anomaly over the Near East. This anomaly is absent in the lower troposphere (Eshel and Farrell 2000; Eshel et al. 2000). Enhanced subsidence at the mid- to upper troposphere might explain some of the differences in precipitation anomalies of this study and Eshel and Farrell (2000) and Eshel et al. (2000) over this region. Our analysis therefore shows that it is important to include the mid- and upper

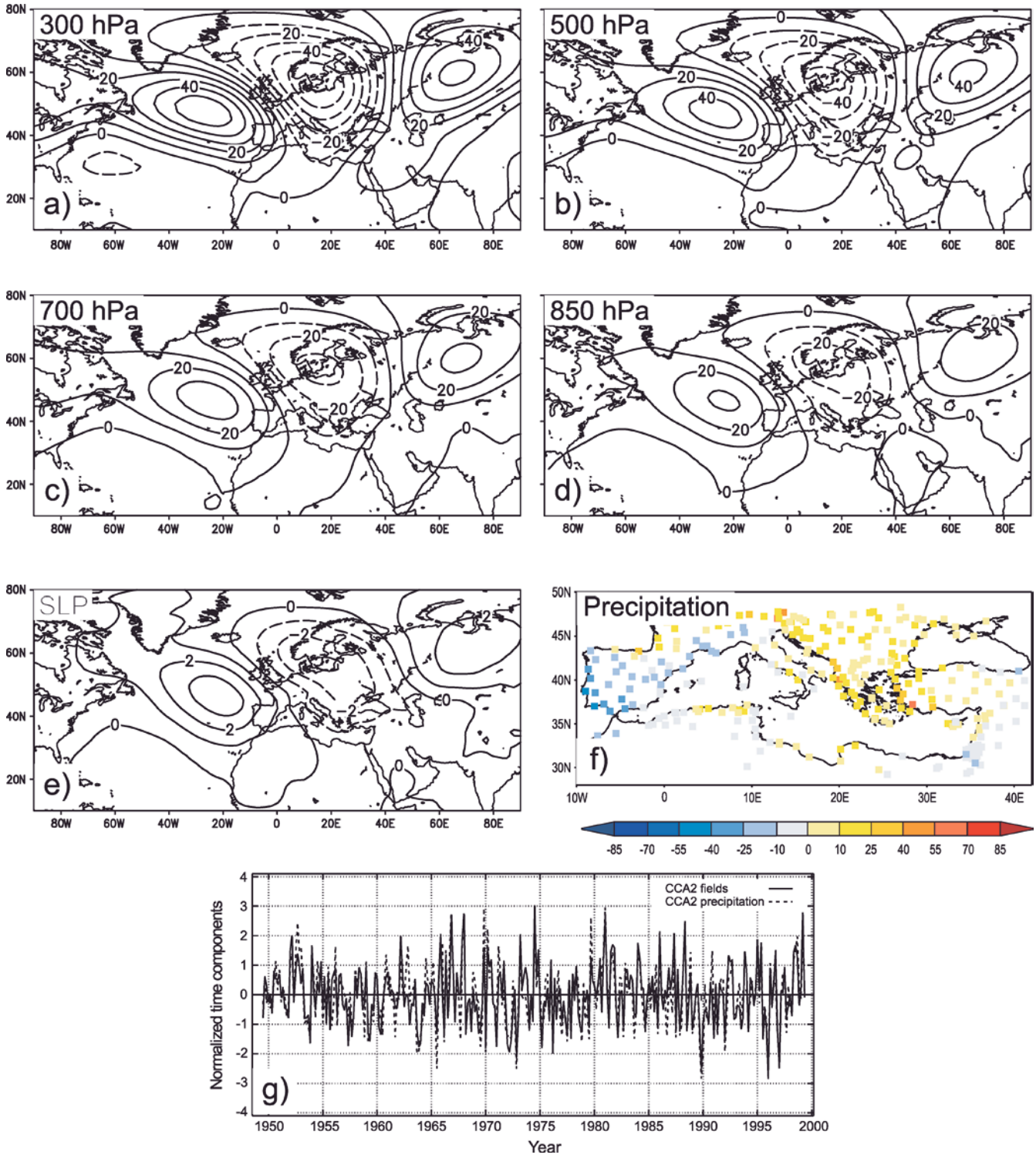

Fig. 4 Canonical spatial patterns of the second CCA. The canonical correlation patterns depict typical anomalies of the variables, with **a** 300 hPa; **b** 500 hPa; **c** 700 hPa; **d** 850 hPa; **e** SLP; **f** wet season precipitation anomalies in mm and **g** normalised time components of CCA2

level large-scale atmospheric circulation in order to explain regional differences in precipitation variability.

The spatial characteristics of the first canonical patterns also agree well with those obtained by Dünkeloh and Jacobeit (2003) for their first winter mode and their second spring canonical component. CCA2 of wet season precipitation (Fig. 4) revealed important large-scale geopotential height anomaly patterns for the larger Mediterranean area. The combination of the large-scale anomalies explains 9.3% of the total October-March

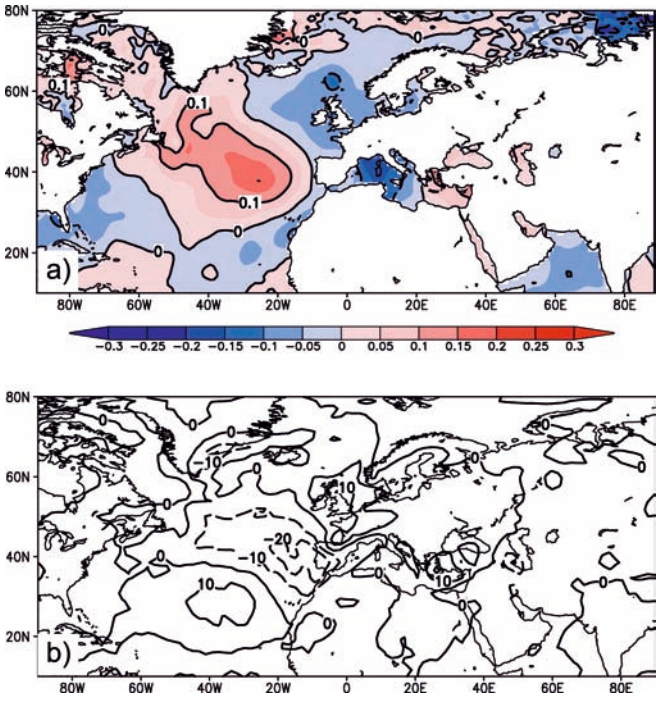

Fig. 5 Regression maps between the second precipitation canonical series shown in Fig. 4g and **a** SST and **b** NCEP reanalysis precipitation for the same period

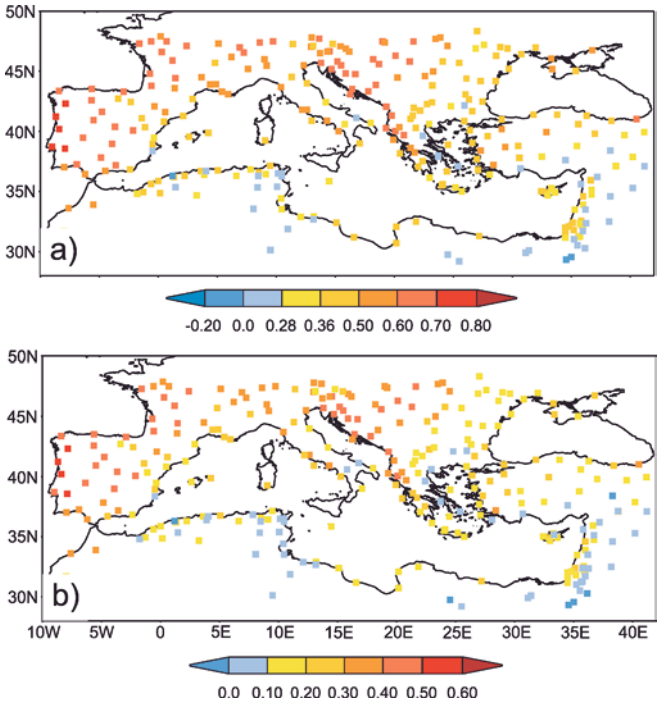

Fig. 6 Spatial distribution of **a** correlation and **b** Brier skill score obtained from cross-validation for the model with five large-scale predictors

Mediterranean precipitation variance. It shows a dipole-like pattern with drier conditions over the Iberian Peninsula and wetter conditions elsewhere (Fig. 4). This seesaw-like oscillation between the western and eastern Mediterranean has already been reported by Kutiel et al. (1996b). The influence of the subtropical high (positive geopotential height anomalies) is restricted to the Iberian Peninsula and northwestern Africa connected with subsidence, stable conditions and reduced precipitation. The areas of enhanced precipitation amounts are located in the southeastern part of the anomalous trough stretching from Greenland over Central Europe to the northern coast of northern Africa. In this sector of the trough, the vorticity advection is maximal connected with strong uplift, instability, condensation and a high chance of precipitation. It has to be pointed out, that the various processes act and interact on different time scales, thus on seasonal averaged charts presented here higher frequency processes are hardly detectable. Eshel (2002) further attributes winter precipitation variability over the eastern Mediterranean to redistribution of heat by the prevailing lateral and vertical air motions.

The second CCA canonical series does not show an intense link to any of the typical large-scale circulation modes. There is however, some significant correlation (–0.42) with the POL (Polar/Eurasia; Barnston and Livezey 1987) pattern.

The efficiency of the statistical model used herein benefits mostly from the contribution of the two CCAs. The correlation and Brier score maps in Fig. 6 show a spatial distribution very similar to the precipitation pattern of the first canonical mode (Fig. 2f). The skill attained with this statistical model is higher where the patterns of the CCA modes (mostly the first one) show the highest loadings. This is a reasonable behaviour since at these sites, the canonical modes explain more variability and therefore a higher fraction of precipitation variability can be predicted with this approach (Xoplaki et al. 2003a). Figure 6 also highlights the fact that the statistical model captures precipitation variability over the whole Mediterranean basin with a lower skill. This limitation has been recognised in other regional studies within the Mediterranean (Zorita et al. 1992; González-Rouco et al. 2000). These results suggest that the inclusion of upper level predictors do not improve the predictability in some areas such as the southeastern Mediterranean coasts or the east coasts of the Iberian Peninsula. We speculate that improved predictability could be achieved by including other large-scale predictors such as moisture advection (Fernández et al. 2003), using statistical models specifically optimised for the critical regions or through other statistical models based on alternative methodologies like analogues or neural network approaches (Zorita and von Storch 1999). Consequently, scenario downscaling using statistical models comparable to the one presented here could be less accurate for areas of low predictability. Some tests have been made with the present approach allowing for a higher number of CCA modes and trying to optimise predictions for areas with low skill. However, results did not present any significant improvement. Thus, more effort towards improving predictability for such areas is needed.

5.2 Long-term trends

Concerning decadal and long term trends, both CCA modes seem to have contributed to the low precipitation records in the late 1980s and early 1990s. However, the first mode is more in agreement with changes in precipitation shown in Fig. 1e. Both the long-term decreasing trends and the dry periods in late 1950s, early 1970s, late 1980s and 1990s as well as the wet transitions in 1960s and late 1970s-early 1980s agree well with the changes in the canonical series of the first mode (correlation 0.72 between both time series). A natural question to ask given the relatively short analysis period is whether the relationships are persistent before the 1950s. Figure 7 gives some insight into this. Figure 7a presents the starting dates of all stations. Sites in the southeast and in general along North Africa have shorter time series. Figure 7b shows standardised averages (4-year moving averages) of all stations with continuous measurements back to 1950 (RR 1950), to 1900 (RR 1900) and back to 1850 (RR 1850). In order to have a comparable scale, standardised averages were calculated normalising the time series by their variance during the period October 1949–March 1999. RR 1950 was calculated using the 292 time series during the 1950–1999 period and thus represents a standardised version of Fig. 1e. RR 1900 (RR 1850) was created using the available records of 110 (12) sites over the period 1900–1999 (1850–1999); it correlates 0.88 (0.65) with RR 1950 in the overlapping period. RR 1900 and RR 1850 correlate 0.74 through the overlapping period (all correlations significant at the 0.05 level). The three time series agree in depicting the wet and dry intervals in the 1950–1999 period as well as the decreasing precipitation trends. For the first half of the twentieth century RR 1900 and RR 1850, in spite the fewer stations, agree well indicating the relatively dry (early 1900s, early 1920s and 1940s) and wet periods (1910s and 1930s). RR 1900 and RR 1850 suggest that the decreasing trend highlighted in Fig. 1e and by RR 1950 is not part of a longer period trend but a feature of the second half of the twentieth century and that the 1960s and late 1970s were actually the wettest intervals since the 1850s.

Some support for this reasoning can be found in the evolution of the large-scale circulation during the twentieth century shown in Fig. 8. Since the NCEP/NCAR reanalysis dataset cannot provide information before 1948, the NCAR SLP dataset (Trenberth and Paolino 1980) was used. The time series labelled as Cs1 and Cs2 (Fig. 8) show the regressed time series (4-year moving average filter) between the SLP dataset (1900 to 1999) and the SLP patterns in Figs. 2e and 4e,

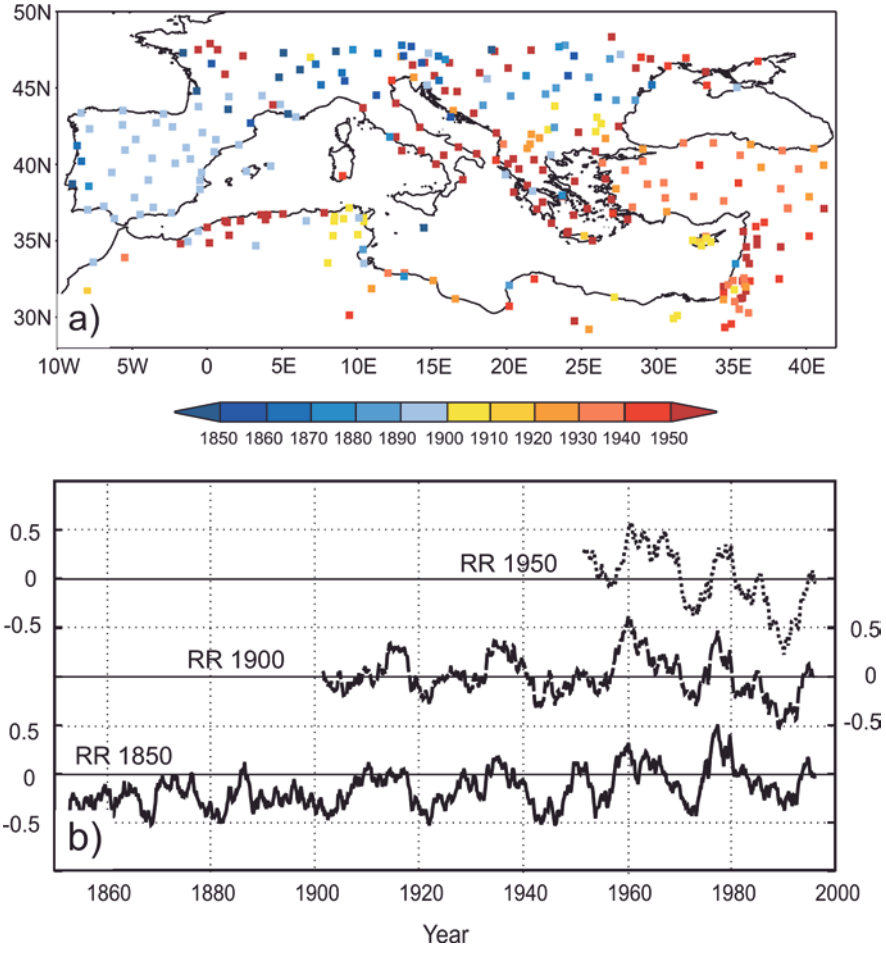

Fig. 7 **a** Dates (decades) of beginning of precipitation records. **b** Spatial averages of precipitation anomalies over all sites with available data for the periods 1850–1999, 1900–1999 and 1950–1999. Time series are normalised to unit standard deviation during the interval 1950–1999

respectively. Prior to this step, the canonical patterns were interpolated to the same resolution (5° × 5° latitude-longitude) as the SLP dataset. The time series shown in Fig. 8 are all normalised by their standard deviation over the period 1950 to 1999. Cs1 and Cs2 can be considered as an estimation with minimum error of the intensities of the canonical series in Figs. 2g and 4g through the entire twentieth century using the information provided by the SLP dataset. It becomes quite apparent that Cs1 and RR 1900 show similar decadal changes since the beginning of the twentieth century (correlation 0.76). For Cs2, this is not the case (correlation 0.06). These results support the idea that the model illustrated in Fig. 2 is stable in time through the first half of the twentieth century. For comparison reasons, Fig. 8 shows also the Gibraltar-Iceland NAO index (Jones et al. 1997) with reversed sign (-NAO). The correlation of this time series with Cs1 is 0.70, suggesting that the long-term changes experienced by the first CCA mode are basically influenced by the NAO. After (before) 1960, both Cs1 and -NAO show negative (positive) trends supporting the idea that the negative precipitation trends after the 1950s are dynamically induced and a feature of the second half of the twentieth century. Comparison of the NAO index and RR 1850 for the second half of the nineteenth century also shows good agreement. These results suggest that wet season Mediterranean precipitation increased since the second half of the nineteenth century and experienced a downward trend through the second half of the twentieth century.

A relevant matter is the possible changes in intensity and frequency of circulation modes affecting Mediterranean precipitation under global climate change. Some model results indicate that the AO and the related NAO tend to become stronger in the future (Paeth and Hense 1999; Gillett et al. 2002; Zorita and González-Rouco 2002; Osborn 2004 and references therein). Our results on decreasing Mediterranean precipitation trends for the second half of the twentieth century would be consistent with this expectation. Additionally, recent findings of idealised SST anomaly experiments by Hoerling et al. (2004) and Hurrell et al. (2004), indicate that SST variations have significantly controlled the North Atlantic circulation, related to the NAO, with the warming of the tropical Indian and western Pacific Ocean being of particular importance. It is however premature to derive a direct relationship of the late twentieth century precipitation trends with predictions of future scenarios since these interdecadal changes could be related to natural variability. In this context, an assessment of how the relevant modes of large-scale variability are simulated by AOGCMs as well as the time stability of their relationship to regional precipitation is desirable.

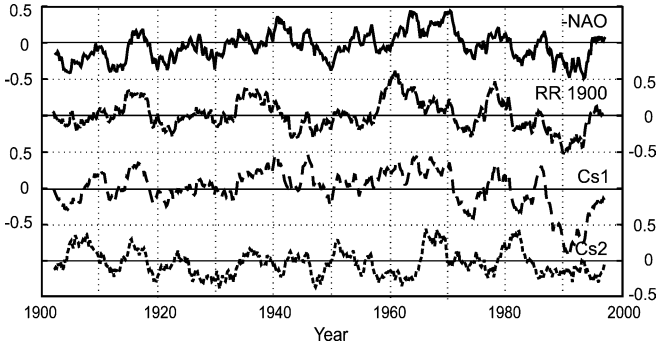

Fig. 8 NAO: Gibraltar-Iceland NAO index (Jones et al. 1997) with reversed sign. RR 1990: spatial average over all sites with available data for the period 1900–1999. Cs1, Cs2: regressed time series (4-years moving average filter) between the NCAR SLP dataset (Trenberth and Paolino 1980) and the SLP patterns in Figs. 2e and 4e, respectively

5.3 NCEP/NCAR reanalysis precipitation

The NCEP/NCAR reanalysis precipitation data have a lower spatial resolution than the station based maps in Figs. 2f and 4f. However, the regression maps shown in Figs. 3b and 5b can provide some information about the spatial extension of the instrumental precipitation canonical vectors (Figs. 2f and 4f). The NCEP precipitation dataset is able to reproduce the main features of the spatial distribution and variability of instrumental precipitation shown in Fig. 1. There is however, a clear underestimation also revealed by the smaller loadings in Figs. 3b and 5b in comparison to Figs. 2f and 4f, respectively. This underestimation can be justified by the coarse resolution, the orography factor, as well as the limitations in the parametrisations of sub-grid scale processes by the models used to produce the reanalysis (Kalnay et al. 1996). In spite of these limitations, there is a significant amount of evidence that certifies the realistic performance of the reanalysis model in reproducing the large-scale characteristics of precipitation (Mo and Higgins 1996; Higgins et al. 1996; Gutowski et al. 1997; Janowiak et al. 1998; Widmann and Bretherton 2000). Widmann et al. (2003) showed that the NCEP precipitation can be successfully downscaled to local precipitation. Our results support the idea that the reanalysis can reproduce large-scale features of precipitation.

5.4 The role of SSTs

It has been proposed that SST anomalies govern, at least partly, precipitation anomalies in neighbouring continental regions (e.g. Hunt and Gordon 1988; Zorita et al. 1992; Reddaway and Bigg 1996; Rimbu et al. 2001; Xoplaki et al. 2000, 2003b). In addition, there are strong indications that fluctuations in SSTs, and hence fluctuations of surface fluxes, are intimately involved in decadal-scale climate variability (Trigo et al. 2000). The almost enclosed Mediterranean Sea represents an important source of energy and moisture for the atmosphere since local evaporation largely exceeds precipitation in all seasons and the characteristics of the local water budget influences the amount of moisture available for the surrounding land regions, especially

northeast Africa and the Middle East (Peixoto et al. 1982; Ward 1998). Thus, the fluctuations of surface heat fluxes are also important for cyclone development (Bartzokas et al. 1994; Trigo et al. 1999). In addition, Zorita et al. (1992) found that the large-scale North Atlantic SST anomalies and the Iberian winter precipitation anomalies are related to each other only indirectly and are both forced by the large-scale state of the atmosphere. In agreement with this idea, the results shown in Table 1 for the Mediterranean SST as a single predictor for Mediterranean precipitation indicate that only 7% of the total October-March Mediterranean precipitation variability can be accounted for. SSTs are influenced by SLP anomalies and in the presence of anomalous cyclonic flow in the atmosphere, the SSTs should respond with net cooling equatorward and westward of the cyclone and a net heating northward and eastward of it. Comparison of Figs. 2e and 4e with Figs. 3a and 5a shows partial agreement with this idea. However, comparison of the geopotential height anomalies in Figs. 2 and 4 with the SST regression maps reveals a direct barotropic overlapping of geopotential height anomalies over SST anomalies. Since the tropospheric structure dominates over a much larger area than the sea anomaly pattern, it can be suggested that the atmosphere seems to be the forcing agent. A simple explanation for this could be the radiative forcing of SST anomalies: increased stability and clear sky conditions in the high geopotential height anomaly areas favours maximum insolation and warming of SSTs.

6 Conclusions

In this study, the relationship between the precipitation variability during the Mediterranean wet season (October-March) and the state of the large-scale atmospheric circulation was investigated for the period 1950–1999.

The CCA experiments with the combined, multi-component large-scale predictors and precipitation investigate the co-variability between geopotential height at different levels and the Mediterranean recording stations wet season precipitation. Approximately 30% of the Mediterranean wet season precipitation variability can be explained linearly by the combination of the five atmospheric predictor fields over the second half of the twentieth century. Using SST as a predictor did not improve the performance of the model for the entire Mediterranean. The skill obtained with SSTs as a single predictor was lower than that calculated with the large-scale atmospheric variables.

The first CCA mode that correlates with the negative NAO/AO and the negative EA/WRUS, is connected with above normal precipitation over most of the Mediterranean region with highest values at the western coasts of the peninsulas and lowest at the southeastern part of the basin. This expression of the first canonical mode could be interpreted as southward shifts of storm tracks from Western Europe towards the Mediterranean and vice-versa that in combination with the local cyclogenesis produce the dipole precipitation pattern.

The downscaling model shows good skill in the western and northern Mediterranean areas. This skill diminishes to the south and especially to the southeast. Thus, more work is needed to develop the precipitation predictability, with either a different set of predictors or a different methodology. An implication of the low skill is that regional scenario precipitation predictions derived with downscaling methods comparable to our approach should be treated with caution in these regions.

The analysis of precipitation trends for the 1950 to 1999 period and back to the middle of the nineteenth century reveals that wet season precipitation increased in the Mediterranean since the mid- nineteenth century with a maximum in the 1960s and decreased since then. Single wet periods occurred in the late 1970s, early 1980s and late 1990s. The second half of the twentieth century shows a general downward trend of 2.2 $mm \cdot month^{-1} \cdot decade^{-1}$. In particular the end of the 1980s-early 1990s are well known for general drought conditions over large parts of the Mediterranean. The first canonical mode has been found to be responsible for the decadal and long term variations in precipitation. These decadal and long-term trends follow those of the Gibraltar-Iceland NAO, thus results suggest that long-term changes in Atlantic variability govern Mediterranean precipitation.

The patterns describing the NCEP/NCAR reanalysis precipitation mean state and variability as well as the CCA-regression maps show that in spite of the underestimation of the maxima and minima the large-scale structure of spatial patterns are well captured.

Although large-scale atmospheric features account for a rather high amount of overall Mediterranean variation, smaller scale processes also influence regional rainfall variability. Land-sea effects and interactions, the influence of the SSTs connected with latent and sensible heat flux, orographical features and thermodynamical aspects interact with each other on different time scales and are superimposed on the quasi-stationary planetary waves which control large-scale advection.

Acknowledgements The authors wish to express their thanks to the following institutions or persons, who kindly provided their valuable instrumental time series, through which the climate analysis for the Mediterranean region was made possible (in alphabetical order of the countries). **Albania**: Prof. Sanxhaku, Academy of Sciences, Hydrometeorological Institute, Tirana; **Algeria**: Dr. M. Kadi, Office National de la Météorologie Climate Center, Dar el Beida, Alger; **Austria**: Drs. I. Auer, R. Böhm and W. Schöner, Zentralanstalt für Meteorologie und Geodynamik (ZAMG), HOHE WARTE 38, Vienna; **Bosnia-Herzegovina**: Dr. E. Sarac, Federal Meteorological Institute, Sarajevo; **Bulgaria**: National Institute of Meteorology and Hydrology, Bulgarian Academy of Sciences, Sofia and D. Lister, Climatic Research Unit, University of East Anglia, Norwich; **Croatia**: Dr. M. Gajic-Capka, Meteorological and Hydrological Service of Croatia, Department for Meteorological Research, Zagreb; **Cyprus**: Dr. L. Hadjioannou, Ministry of Agriculture, Natural Resources and Environment, Meteorological Service, Nicosia; **Greece**: Hellenic National Meteorological Service, Hellinikon, Athens; **Israel**: Dr. A. Porat,

Ministry of Transport, Israel Meteorological Service; Bet Dagan; **Italy**: Colonel Dr. M. Capaldo, Aeronautica Militare, Centro Nazionale di Meteorologia e Climatologia Aeronautica Aeroporto Pratica di Mare, Pomezia; **Jordan**: Dr. H. AL Sha'er, The Hashimite Kingdom of Jordan, Meteorological Department Climate Division Amman Civil Airport, Amman; **Lebanon**: Dr. A. Bejjani, Republic of Lebanon, Ministry of Transport, Meteorological Services, International Airport of Beyrouth, Beyrouth; **Libya**: Dr. K. Elfadli, Libyan Meteorological Department, Climatological and Agrometeorological Section, Tripoli; **Moldavia**: Dr. L. Fisher, Hidrometeo Service (Chimet), Chisinau; **Romania**: Dr. A. Busuioc, National Institute of Meteorology and Hydrology, Bucharest; **Skopje**: Dr. N. Aleksovska, Hydrometeorological Institute of the FYR Macedonia, Meteorological and Climatological division, Skopje; **Slovenia**: Dres. T. Ovsenik-Jeglié, J. Miklavçiç and B. Zupani, Hydrometeorological Institute of Slovenia, Ministry of the environment and Physical Planning, Ljubliana; **Spain**: Universidad Computense de Madrid, Madrid; **Switzerland**: Swiss Meteorological Office, (SMA MeteoSchweiz), Zurich **Tunisia**: Dr. M. Ketata and Prof. H. Hajji, République tunesienne, Ministére de Transport, Institute National de la Météorologique, Tunis-Carthage. For Egypt, France, Hungary, Malta, Morocco, Portugal, Serbia, Syria and Turkey the data have been obtained from the GHCN (Global Historical Climatology Network) version 2b and/or where kindly provided by the German Meterological Service (DWD), Geschäftsfeld Seeschifffahrt and David Lister, Climatic Research Unit, University of East Anglia, Norwich, UK. Tommaso Abrate, Department of Hydrology and Water Resources, WMO, Geneva, Switzerland, provided us with addresses and relevant information on how to contact the responsible persons and institutions from the different countries. We also thank NCEP/NCAR for providing their reanalysis data. We are indebted to the British Meterological Office for the preparation of the gridded SST data. Dr. Elena Xoplaki was partially supported by Fifth Framework Programme of the European Union (project SOAP); Dr. J. Fidel González-Rouco was partially funded by project REN-2000-0786-cli and REN-2002-04584-C04-01-CLI; Dr. Jürg Luterbacher was supported by the Swiss Science Foundation (NCCR Climate). The authors wish to thank the Marchese Francesco Medici del Vascello Foundation for financial support. We thank Paul Della-Marta for proofreading the English text. The authors thank Dr. Gidon Eshel and an anonymous reviewer for their constructive comments on this manuscript.

References

Barnett TP, Preisendorfer RW (1987) Origins and levels of monthly and seasonal forecast skill for United States air temperature determined by canonical correlation analysis. Mon Weather Rev 115: 1825–1850

Barnston AG, Livezey RE (1987) Classification, seasonality and persistence of low frequency atmospheric circulation patterns. Mon Weather Rev 115: 1825–1850

Bartzokas A, Metaxas DA, Ganas IS (1994) Spatial and temporal sea-surface temperature covariances in the Mediterranean. Int J Climatol 14: 201–213

Buffoni L, Maugeri M, Nanni T (1999) Precipitation in Italy 1833 to 1996. Theor Appl Climatol 63: 33–40

Buffoni L, Maugeri M, Nanni T (2000) Variation of temperature and precipitation in Italy from 1866 to 1995. Theor Appl Climatol 65: 165–174

Busuioc A, von Storch H (1996) Changes in the winter precipitation in Romania and its relation to the large scale circulation. Tellus 48A: 538–552

Busuioc A, von Storch H, Schnur R (1999) Verification of GCM-generated regional seasonal precipitation for current climate and of statistical downscaling estimates under changing climate conditions. J Clim 12: 258–272

Corte-Real J, Zhang X, Wang X (1995) Large-scale circulation regimes and surface climatic anomalies over the Mediterranean. Int J Climatol 15: 1135–1150

Cubasch U, Meehl GA, Boer GJ, Stouffer RJ, Dix M, Noda A, Senior CA, Raper S, Yap KS (2001) Projections of future climate change. In: Houghton JT, Ding Y, Griggs DJ, Noguer M, van der Linden PJ, Xiaoxu D (eds) Chapter 9 of climate change 2001; the scientific basis. Contribution of Working Group I to the Third Assessment Report of the Intergovernmental Panel on Climate Change (IPCC). Cambridge University Press, Cambridge, UK, pp 99–181

Dünkeloh A, Jacobeit J (2003) Circulation dynamics of Mediterranean precipitation variability 1948–98. Int J Climatol 23: 1843–1866

Easterling DR, Karl TR, Gallo KP, Robinson TA, Trenberth KE, Dai AG (2000) Observed climate variability and change of relevance to the biosphere. J Geophys Res 105: 20,101–20,114

Edwards AL (1984) An introduction to linear regression and correlation, 2nd edn. Freeman WH, New York, pp 81–83

Eshel G (2002) Mediterranean climates. Isr J Earth Sci 51: 157–168

Eshel G, Farrell BF (2000) Mechanisms of Eastern Mediterranean rainfall variability. J Atmos Sci 57: 3219–3232

Eshel G, Cane MA, Farrell BF (2000) Forecasting Eastern Mediterranean drought. Mon Weather Rev 128: 3618–3630

Esteban-Parra MJ, Rodrigo FS, Castro-Diez Y (1998) Spatial and temporal patterns of precipitation in Spain for the period 1880–1992. Int J Climatol 14: 1557–1574

Fernández J, Saenz J, Zorita E (2003) Analysis of wintertime atmospheric moisture transport and its variability over Southern Europe in the NCEP-Reanalyses. Clim Res 23: 195–215

Folland CK, Karl TP, Christy JR, Clarke RA, Gruza GV, Jouzel J, Mann ME, Oerlemans J, Salinger MJ, Wang SW (2001) Observed climate variability and change. In: Houghton JT, Ding Y, Griggs DJ, Noguer M, van der Linden PJ, Xiaoxu D (eds) Chapter 2 of climate change 2001; the scientific basis. Contribution of Working Group I to the Third Assessment Report of the Intergovernmental Panel on Climate Change (IPCC). Cambridge University Press, Cambridge UK, pp 99–181

Fotiadi AK, Metaxas DA, Bartzokas A (1999) A statistical study of precipitation in northwest Greece. Int J Climatol 19: 1221–1232

Gibelin A-L, DéquéM (2003) Anthropogenic climate change over the Mediterranean region simulated by a global variable resolution model. Clim Dyn 20: 327–339 DOI 10.1007/s00382-002-0277-1

Gillett NP, Allen MR, McDonald RE, Senior CA, Shindell DT, Schmidt GA (2002) How linear is the Arctic Oscillation response to greenhouse gases? J Geophys Res 107 DOI:10.1029/2001JD000589

Giorgi F (2002a) Variability and trends of sub-continental scale surface climate in the twentieth century. Part I: observations. Clim Dyn 18: 675–691 DOI 10.1007/s00382-001-0204-x

Giorgi F (2002b) Variability and trends of sub-continental scale surface climate in the twentieth century. Part II: AOGCM simulations. Clim Dyn 18: 693–708 DOI 10.1007/s00382-001-0205-9

Giorgi F, Francisco R (2000a) Uncertainties in regional climate change predictions. A regional analysis of ensemble simulations with the HADCM2 AOGCM. Clim Dyn 16: 169–182

Giorgi F, Francisco R (2000b) Evaluating uncertainties in the prediction of regional climate change. Geophys Res Lett 27: 1295–1298

González-Rouco JF, Heyen H, Zorita E, Valero F (2000) Agreement between observed rainfall trends and climate change simulations in Southern Europe. J Clim 13: 3057–3065

González-Rouco JF, Jimenez JL, Quesada V, Valero F (2001) Quality control and homogenization of monthly precipitation data in the southwest of Europe. J Clim 14: 964–978

Gutowski WJ Jr, Chen Y, Ötles Z (1997) Atmospheric water vapor transport in NCEP-NCAR reanalyses: comparison with river discharge in the central United States. Bull Am Meteorol Soc 78: 1957–1969

Higgins RW, Mo KC, Schubert SD (1996) The moisture budget of the central United States as evaluated in the NCEP/NCAR and the NASA/DAO reanalyses. Mon Weather Rev 124: 939–963

Hoerling MP, Hurrell JW, Xu T, Bates GT, Phillips A (2004) Twentieth century North Atlantic climate change. Part II: Understanding the effect of Indian Ocean warming. Clim Dyn (in press)

Hulme M, Barrow EM, Arnell NW, Harrison PA, Johns TC, Downing TE (1999) Relative impacts of human-induced climate change and natural variability. Nature 397: 688–691

Hunt B, Gordon H (1988) The problem of naturally occurring drought. Clim Dyn 3: 19–33

Hurrell JW (1995) Decadal trends in the North Atlantic Oscillation: regional temperatures and precipitation. Science 269: 676–679

Hurrell JW, Hoerling MP, Phillips A, Xu T (2004) Twentieth century North Atlantic climate change. Part I: Assessing determinism. Clim Dyn (in press)

IPCC (2001) Climate change 2001: the scientific basis. Contribution of Working Group I to Third Assessment Report of the Intergovernmental Panel on Climate Change. Houghton, JT, Ding Y, Griggs DJ, Noguer M, van der Linden PJ, Dai X, Maskell K, Johnson CA (eds) Cambridge University Press, Cambridge, UK and New York, NY, USA

Jacobeit J (2000) Rezente Klimaentwicklung im Mittelmeerraum. Petermanns Geogr Mittl 144: 22–33

Janowiak JE, Gruber A, Kondragunta CR, Livezey RE, Hufman GJ (1998) a comparison of the NCEP-NCAR reanalysis precipitation and the GPCP rain gauge-satellite combined dataset with observational error considerations. J Clim 11: 2960–2979

Jones PD, Jonsson T, Wheeler D (1997) Extension to the North Atlantic Oscillation using early instrumental pressure observations from Gibraltar and Southwest Iceland. Int J Climatol 17: 1433–1450

Jones PD, Mann ME (2004) Climate over past millennia. Rev Geophys 42. RG2002 DOI 10.1029/2003RG000143

Kadioğlu M (2000) Regional variability of seasonal precipitation over Turkey. Int J Climatol 20: 1743–1760

Kadioğlu M, Tulunay Y, Borhan Y (1999) Variability of Turkish precipitation compared to El Nio events. Geophys Res Lett 26: 1597–1600

Kalnay et al. (1996) The NCEP/NCAR 40-Year Reanalysis Project. Bull Am Meteorol Soc 77: 437–471

Karaca M, Deniz A, TayançM (2000) Cyclone track variability over Turkey in association with regional climate. Int J Climatol 20: 1225–1236

Kistler R et al. (2001) The NCEP-NCAR 50-year Reanalysis: monthly means CD-ROM and documentation. Bull Am Meteorol Soc 82: 247–267

Knippertz P, Christoph M, Speth P (2002) Long-term precipitation variability in Morocco and the link to the large-scale circulation in recent and future climates. Meteorol Atmos Phys DOI 10.1007/s00703-002-0561-y

Kutiel H, Maheras P, Guika S (1996a) Circulation indices over the Mediterranean and Europe and their relationship with rainfall conditions across the Mediterranean. Theor Appl Climatol 54: 125–138

Kutiel H, Maheras P, Guika S (1996b) Circulation and extreme rainfall conditions in the eastern Mediterranean during the last century. Int J Climatol 16: 73–92

Livezey RE, Smith TM (1999) Considerations for use of the Barnett and Preisendorfer (1987) algorithm for canonical correlation analysis of climate variations. J Clim 12: 303–305

Maheras P (2000) Synoptic situations causing drought in the Mediterranean basin. In: Vogt JV, Somma F (eds) Drought and drought mitigation in Europe. Kluwer Academic, pp 91–102

Mariotti A, Struglia MV (2002) The hydrological cycle in the Mediterranean region and implications for the water budget of the Mediterranean Sea. J Clim 15: 1674–1690

Matulla C, Scheifinger H, Menzel A, Koch E (2003) Exploring two methods for statistical downscaling of Central European phenological time series. Int J Biometeorol 48:56–64 DOI 10.1007/s00484-003-0186-y

Michaelsen J (1987) Cross-validation in statistical climate forecast models. J Clim Appl Meteor 26: 1589–1600

Mo KC, Higgins RW (1996) Large-scale atmospheric moisture transport as evaluated in the NCEP/NCAR and the NASA/DAO reanalyses. J Clim 9: 1531–1545

New MG, Hulme M, Jones PD (2000) Representing twentieth-century space time climate fields. Part II: development of a 1901–1996 mean monthly terrestrial climatology. J Clim 13: 2217–2238

New M, Todd M, Hulme M, Jones P (2001) Precipitation measurements and trends in the twentieth century. Int J Climatol 21: 1899–1922

Nicholls N, Gruza GV, Jouzel J, Karl TR, Ogallo LA, Parker DE (1996) Observed Climate variability and change. In: Houghton JT, Meira Filho LG, Callander BA, Harris N, Kattenberg A, Maskell K (eds) Chapter 3 of climate change 1995; the science of climate change, Contribution of Working Group I to the Second Assessment Report of the Intergovernmental Panel on Climate Change (IPCC). Cambridge University Press, Cambridge, UK, pp 133–192

North GR, Moeng FJ, Bell TL, Cahalan RF (1982) The latitude dependence of the variance of zonally averaged quantities. Mon Weather Rev 110: 319–326

Osborn TJ (2004) Simulating the winter North Atlantic Oscillation: the roles of internal variability and greenhouse gas forcing. Clim Dyn DOI 10.1007/s00382-004-0405-1

Paeth H, Hense A, Glowienka-Hense R, Voss R, Cubasch U (1999) The North Atlantic Oscillation as an indicator for greenhouse gas induced regional climate change. Clim Dyn 15: 953–960

Peixoto JP, De Almeida M, Rosen RD, Salstein DA (1982) Atmospheric moisture transport and the water balance of the Mediterranean Sea. Water Resour Res 18: 83–90

Peterson TC, Vose RS, Schmoyer R, Razuvaëv V (1998) Global historical climatology network (GHCN) quality control of monthly temperature data. Int J Climatol 18: 1169–1179

Piervitali E, Colacino M, Conte M (1998) Rainfall over the central-western Mediterranean Basin in the period 1951–1995. Part I: precipitation trends. Il Nuovo Cimento 21C: 331–344

Quadrelli R, Pavan V, Molteni F (2001) Wintertime variability of Mediterranean precipitation and its links with large-scale circulation anomalies. Clim Dyn 17: 457–466

Rayner NA, Horton EB, Parker DE, Folland CK, Hackett RB (1996) Version 2.2 of the Global Sea-Ice and Sea Surface Temperature Data Set, 1903–1994. Climate Research Technical Note 74, unpublished document available from Hadley Centre

Reddaway JM, Bigg GR (1996) Climatic change over the Mediterranean and links to the more general atmospheric circulation. Int J Climatol 16: 651–661

Rimbu N, le Treut H, Janicot S, Boroneant C, Laurent C (2001) Decadal precipitation variability over Europe and its relation with surface atmospheric circulation and sea surface temperature. Q J R Meteorol Soc 127: 315–329

Rodrigo FS (2002) Changes in climate variability and seasonal rainfall extremes: a case study from San Fernando (Spain), 1821–2000. Theor Appl Climatol 72: 193–207

Thompson DWJ, Wallace JM (1998) The Arctic Oscillation signature in the wintertime geopotential height and temperature fields. Geophys Res Lett 25: 1297–1300

Tomozeiu R, Lazzeri M, Cacciamani C (1995) Precipitation fluctuations during the winter season from 1960 to 1995 over Emilia-Romagna, Italy. Theor Appl Climatol 72: 221–229

Trenberth K, Paolino DA (1980) The Northern Hemisphere sea-level pressure data set: trends, errors and discontinuities. Mon Weather Rev 108: 855–872

Trigo IF, Davies TD, Bigg GR (1999) Objective climatology of cyclones in the Mediterranean Region. J clim 12: 1685–1696

Trigo IF, Davies TD, Bigg GR (2000) Decline in Mediterranean rainfall caused by weakening of Mediterranean cyclones. Geophys Res Lett 27: 2913–2916

TürkesM (1998) Influence of geopotential heights, cyclone frequency and southern oscillation on rainfall variations in Turkey. Int J Climatol 18: 649–680

von Storch H, Zwiers FW (1999) Statistical analysis in climate research. Cambridge University Press, UK

von Storch H, Zorita E, Cubasch U (1993) Downscaling of global climate change estimates to regional scales: an application to Iberian rainfall in wintertime. J Clim 6: 1161–1171

Vose RS, Schmoyer RL, Steurer PM, Peterson TC, Heim R, Karl TR, Eischeid J (1992) The Global Historical Climatology Network: long-term monthly temperature, precipitation, sea level pressure, and station pressure data. ORNL/CDIAC-53, NDP- 041, Carbon Dioxide Information Analysis Center, Oak Ridge National Laboratory, Oak Ridge, Tennessee, USA

Ward NN (1998) Diagnosis and short-lead predictions of summer rainfall in tropical North Africa at interannual and multidecadal time scales. J clim 11: 3167–3191

Widmann M, Bretherton CS (2000) Validation of mesoscale precipitation in the NCEP reanalysis using a new grid-cell dataset for the northwestern United States. J Clim 13: 1936–1950

Widmann M, Bretherton CS, SalathéEP Jr (2003) Statistical precipitation downscaling over the northwestern United States using numerically simulated precipitation as a predictor. J Clim 16: 799–816

Wilks DS (1995) Statistical Methods in the Atmospheric Sciences: an Introduction. In: Dmowska R, Holton JR (eds) International Geophysics Series, 59. Academic Press

WMO (1986) Guidelines on the quality control of surface climatological data/prepared by Abbott PF (UK) as Rapporteur in the WMO Commission for Climatology. Geneva: WCP, (WCP-85). iv, appendices

Xoplaki E (2002) Climate variability over the Mediterranean. PhD thesis, University of Bern, Switzerland ([http://sinus.unibe.ch/klimet/docs/phd_xoplaki.pdf])

Xoplaki E, González-Rouco JF, Luterbacher J, Wanner H (2003a) Mediterranean summer air temperature variability and its connection to the large-scale atmospheric circulation and SSTs. Clim Dyn 20: 723–739 DOI 10.1007/s00382-003-0304-x

Xoplaki E, González-Rouco FJ, Gyalistras D, Luterbacher J, Rickli R, Wanner H (2003b) Interannual summer air temperature variability over Greece and its connection to the large-scale atmospheric circulation and Mediterranean SSTs 1950–1999. Clim Dyn 20: 523–536 DOI 10.1007/s00382-002-0291-3

Xoplaki E, Luterbacher J, Burkard R, Patrikas I, Maheras P (2000) Connection between the large-scale 500 hPa geopotential height fields and precipitation over Greece during wintertime. Clim Res 14: 129–146

Xu JS (1993) The joint modes of the coupled atmosphere-ocean system observed from 1967 to 1987. J Clim 6: 816–838

Zorita E, González-Rouco JF (2002) Are temperature sensitive proxies adequate for North Atlantic Oscillation reconstructions? Geophys Res Lett 29 DOI 10.1029/2002GL015404)

Zorita E, von Storch H (1999) The analog method as a simple statistical downscaling technique: comparison with more complicated methods. J Clim 12: 2474–2489

Zorita E, Kharin V, von Storch H (1992) The atmospheric circulation and sea surface temperature in the North Atlantic area in winter: their interaction and relevance for Iberian precipitation. J Clim 5: 1097–1108